

## Diffusion and Thermal Shock Behaviour of Silicate Dental Ceramics

Burcu ERTUĞ \*

Faculty of Engineering and Architecture, Nişantaşı University, Maslak Mahallesi, Taşyoncası Sokak, No:1V and No:1Y 34398, Sarıyer-Istanbul, Turkey

<https://doi.org/10.5755/j02.ms.30414>

Received 31 December 2021; accepted 23 May 2022

The purpose of this study is to examine the diffusion and thermal shock behaviour of alternative dental silicates. The samples derived from the BaO-SiO<sub>2</sub> system have been produced by melting process and followed by the heat treatment. X-ray examinations have indicated that the amount of orthorhombic sanbornite phase raised due to treatment temperature as revealed by the peak intensities. The alteration of the morphology by treatment temperature was evident from scanning electron microscopy SEM images. Crystallization at low temperature produced small crystallites and coarsening was not observed with a temperature rise. The failure of the dental samples after the thermal shock test was examined using SEM. A continuous crack geometry and very few crack branching were observed. Diffusivity constant (D) and diffusion rate were examined vs treatment temperature for the present system. Diffusion depth (L) was doubled when the crystallization treatment was applied. Based on the obtained results, these silicate samples might take part in the further characterization studies to be used as alternative dentistry materials.

*Keywords:* dental materials, diffusion, silicate, thermal shock.

### 1. INTRODUCTION

All-ceramic dental materials offer superior aesthetics for the patients [1]. Being similar to natural teeth, lithium disilicate-based materials are used to manufacture crowns, veneers and dental bridges. The fine-grained interlocking crystals in the lithium disilicate provide high mechanical properties for the replacement of the anterior teeth [2]. As a result of their clinical longevity lithium disilicate all-ceramic structures are successful on the commercial scale [3, 4] particularly, for the single crowns. Though the chipping of the veneer is a common obstacle in these materials [5].

Post-failure surface cracks hold potential for propagation until the implant failure [6]. Therefore, many attempts have been made to improve these structures through controlled crystallization [7, 8]. However, detailed knowledge of the heat treatments for the synthesis of the glass-ceramics is scarce. The combination of high thermal expansion coefficient and low thermal conductivity causes all-ceramic materials to be susceptible to thermal shock and the thermal expansion coefficient can be reduced through crystallization [9]. The examination of the surface cracking due to thermal gradient can provide knowledge on fracture behaviour. Some features of these lithium disilicate dental materials that are mentioned above were compared in Table 1 from the previous studies [10–22] in terms of controlled crystallization parameters, microstructural morphology, and dental features.

For the silicate systems, a detailed examination of the diffusion phenomena provides some helpful data to produce the functional materials [23]. There are much experimental data on the diffusion coefficients of different

cations in the silicate glasses that have a critical effect on the glass-ceramic processes. It is known that the number and the mobility of the ions determine the diffusivity. However, the mobility of Si ions is not high whereas that of the alkali ions is considered. The glassy phase in a glass-ceramic material is where the diffusion phenomena take place [24].

The chemical environment of the crystal is influential on the diffusivity. As long as there is a chemical potential gradient, the relevant ion will flux down that potential gradient [25]. The data on the diffusivities as a function of temperature have been plotted for Li, Na, K, Mg, Ca, Sr, Ba and Zn in the aluminosilicate glasses [26]. Also, there are some systematic studies on the alkali diffusivities for the mixed-alkali glasses [27]. In another study, Na diffusivities have been determined in sodium borosilicate, sodium boroaluminosilicate and alkali aluminosilicate glasses [28].

In addition, a lot of diffusion-controlled processes in the oxide materials are strongly dependent on the temperature [24]. The diffusivity versus temperature plots have been shown to be of Arrhenius-type [29]. It is possible to determine the diffusion activation energy and the pre-exponential factor,  $D_0$  by fitting  $\ln D$  versus  $1/T$  data to Arrhenius equation [26]. The diffusivities of two network-modifier ions (Na and Ca) have been shown as an Arrhenius plot for a soda-lime silicate glass [30]. It is also known that thermally activated diffusivities of alkali ions are influenced strongly by the composition of the silicate glasses. For binary alkali silicate glasses, the activation energies related to diffusion have also been calculated [31].

\* Corresponding author. Tel.: +90-212-2101010.  
E-mail: [burcu.ertug@nisantasi.edu.tr](mailto:burcu.ertug@nisantasi.edu.tr) (B. Ertug)

**Table 1.** A comparison of various dental materials for some features

Chemical composition	Controlled crystallization, K/hrs	Crystals	Dental features
Binary and multicomponent lithium silicate	853, 873, 923+1073; 1123 [10]	Nuclei	Dental restoration
TiO <sub>2</sub> -ZrO <sub>2</sub> -Li <sub>2</sub> O-CaO-Al <sub>2</sub> O <sub>3</sub> -SiO <sub>2</sub>	723/1+ 883-1053 [11]	Needle	General dentistry
SiO <sub>2</sub> -Al <sub>2</sub> O <sub>3</sub> -Li <sub>2</sub> O-K <sub>2</sub> O- B <sub>2</sub> O <sub>3</sub> -ZrO <sub>2</sub>	1073-1173/2+1223/4 [12]	Needle	Dental bridge
Li <sub>2</sub> O-SiO <sub>2</sub> -Al <sub>2</sub> O <sub>3</sub> -K <sub>2</sub> O	773K/1/6; 923-973/1/3+123/1/6 [13]	Needle /flake	Highly translucent
Li <sub>2</sub> O-K <sub>2</sub> O-Al <sub>2</sub> O <sub>3</sub> -SiO <sub>2</sub>	823-1173/1 [14]	Dendrite/ Rod	NA
SiO <sub>2</sub> -Li <sub>2</sub> O-Al <sub>2</sub> O <sub>3</sub> -K <sub>2</sub> O-ZrO <sub>2</sub>	793/1/6, at 1013/1/3+ 123/1/6 [15]	Plate	High-strength and translucency
SiO <sub>2</sub> -Li <sub>2</sub> O-K <sub>2</sub> O-ZrO <sub>2</sub>	923, 1023, 1173/1 [16]	Needle /Granular	Dental restoration
SiO <sub>2</sub> -Li <sub>2</sub> O-K <sub>2</sub> O-Al <sub>2</sub> O <sub>3</sub> -ZrO <sub>2</sub>	1223/4 [17]	Small Crystals	Challenging restorations
SiO <sub>2</sub> -Al <sub>2</sub> O <sub>3</sub> -K <sub>2</sub> O-Li <sub>2</sub> O	1073, 1123, 1173/1 [18]	Dendrite/Interlocked	Needs toxicity tests
Lithium disilicate	863-878+1053-1113 [19]	Rod /Needle	Mechanical performance
MnO <sub>2</sub> doped lithium disilicate	973/1 [20]	Elongated	Posterior crowns, inlay-retained bridges
Li <sub>2</sub> O-SiO <sub>2</sub> -ZnO-K <sub>2</sub> O	863-893/3+1033-1143/2 [21]	Elongated	Interlocking crystals
Pressable dental materials	Commercial material [22]	Elongated	Pressable all-ceramics

Thus it is beneficial to study the diffusion in the glass-ceramic systems which in general, contain a small amount of glassy phase. In this study, silicate-based samples have been examined as dental implant materials involving crystallization behaviour, fracture surfaces and diffusion parameters.

## 2. EXPERIMENTAL PROCEDURE

For preparing the samples, the starting materials with technical quality; silicon oxide (SiO<sub>2</sub>) and barium carbonate (BaCO<sub>3</sub>) were used. Powder chemicals, before to the reaction were subjected to drying in an oxide furnace. The calcination was carried out inside an alumina crucible, at 1623 K for the carbonate removal and formation of the disilicate. The complete fusion was achieved at 1823 K. The glass batch was homogenized by pouring the molten glass into the distilled water a couple of times. Final glass samples with diameters of 5 mm. and the lengths of 10 mm. were shaped by the casting method as in Fig. 1.

Later, an annealing stage was applied to these samples and then, they were slowly cooled to room temperature in the furnace. The glass samples were isothermally treated in the range of 983–1198 K. The first set of heat-treated samples were coded as T9060, T0060 and T4060 with different treatment temperatures for a constant time of 1hrs. and the second set of samples was coded as T4030, T4012 and T4018 with a constant temperature of 813 K for

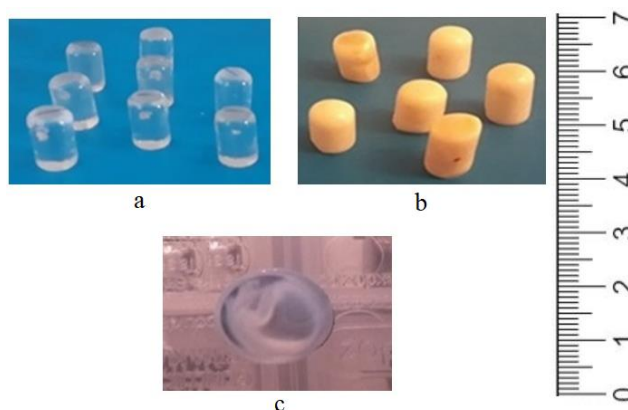


**Fig. 1.** Images of glass samples in the different states: a – vitreous; b – crystallized; c – nucleated states

To examine the precipitated crystals in the microstructure of the glass phase, a scanning electron microscope (SEM) JEOL JSM 6060 was used. For this purpose, various temperature and time combinations were applied and the treated samples for SEM analysis were prepared by metallographic methods. The sample surfaces were etched using an HF solution with a concentration of 5 % for 15–20 s. The surfaces were gold-coated before to microstructural examination. Later, the microstructural phase morphologies were examined using electron scanning microscope.

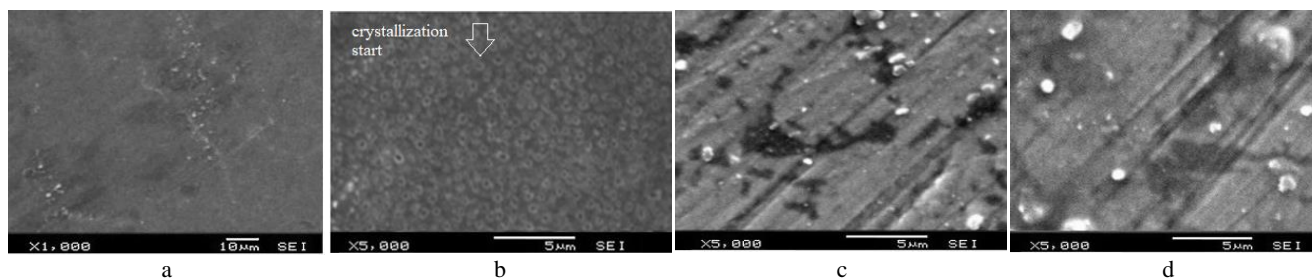


**Fig. 2.** SEM images after: a, b–763 K; c–773 K; d–813 K for 1 h and then firing at different temperatures

The phase purity of the crystallized samples was also examined through X-ray diffractometry (D/max-2200/PC, Rigaku) with Cu-K $\alpha$  radiation ( $\lambda = 1.54056$  nm) at 40 kV and 20 mA using 3 $^\circ$ /min scan rate in the range of 20–40 $^\circ$ .

A thermal shock test was conducted for the sample of T0060. For the simulation of the oral environment, the sample was held for 30 s between the temperatures of 268 K and 328 K in a vertical furnace (Nüve KD 400) to maintain a suitable air flow without applying a cycle. Cold water was used as the quenching environment and after the quenching, the surface failure was analyzed; firstly by examining to see whether there are any surface cracks visible to the naked-eye and then secondly under SEM.

For the dental ceramic-based samples, thermal diffusion parameters were calculated by the given formulas. For the present system diffusivity value,  $D$  was calculated with the Eq. 1 as follows [32]:

$$D = D_0 \cdot \exp E_A/k \cdot T, \quad (1)$$

where,  $D$  is the diffusivity, cm $^2$ /s;  $D_0$  is the material constant ( $8.81 \times 10^{-13}$  cm $^2$ /s);  $E_A$  is the activation energy related to the diffusion of Ba cation ( $-0.72$  eV/atom);  $T$  is the temperature, K;  $k$  is the Boltzmann constant.

The diffusion length of Ba cation,  $L$  has been calculated for different times with the Eq. 2 as follows [33]:

$$L = \sqrt{4 \cdot D \cdot t}, \quad (2)$$

where  $L$  is the diffusion depth;  $D$  is the diffusivity, cm $^2$ /s;  $t$  is the diffusion time, s.

### 3. RESULTS AND DISCUSSION

According to the visual inspection of the cast samples, stoichiometric glasses derived from the binary BaO-SiO $_2$  system are prone to devitrification, even before crystallization treatment as in Fig. 1 c, in which a translucent appearance was clearly observed.

The microstructural examinations pointed out a rise in the content of the dental crystal converting the translucent samples into pale opaque colour. Fig. 2 a and b show the crystallized microstructure after holding at a relatively low nucleation temperature close to glass transition,  $T_g$  point of the composition followed by firing. The high nucleation rate and low crystal growth rate consecutively after the heat treatment produced small crystallites [1], which is known to be adequate for dental implants.

Early crystallization was marked in Fig. 2 b at high magnification. As the samples were treated at a higher nucleation temperature, dark and bright contrast of the crystallized phases were clearly observed in the microstructure. However, the rise of the nucleation temperature did not reveal an observable microstructural coarsening. On the other hand, the duration of the heat treatment contributed effectively to the microstructural evolution in that the crystallized phases became more evident after a longer heat treatment time.

The samples contained a higher amount of the main crystal phase Ba $_2$ Si $_2$ O $_5$  crystallized from the glassy matrix as the treatment temperature raised. After the crystal growth process, the dental ceramics reached its final

crystallized state with a full silicate phase. During the preparation of the glass samples, inside the matrix, a certain amount of crystal formation was observed. Since relatively low temperatures close to the glass-transition are known to induce the nucleation process, the first stage of the treatment was carried out at around the  $T_g$  of our sample (763 K). As can be seen in Fig. 3., after the treatment at a constant temperature, the main phase of orthorhombic sanbornite structure was observed with the JCPDS card number 01-071-1441 and the lattice constants of  $a = 7.69$  Å,  $b = 13.52$  Å and  $c = 4.63$  Å. As the heat treatment time extended from 1 to 3 h, the peak intensities increased as well due to a rise in the content of the main crystalline phase.

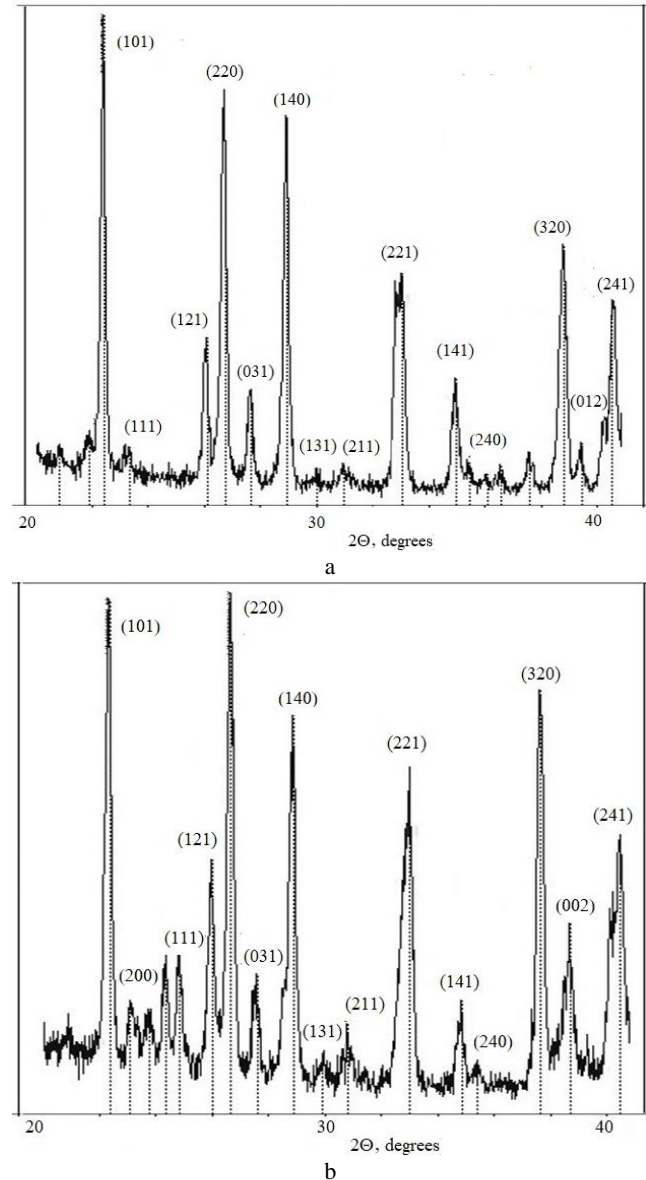


**Fig. 3.** XRD patterns of samples: a–T4060; b–T4018

In a previous study, barium disilicate was synthesized using the sol-gel method [34] where the crystallization behaviour of the sample by the sol-gel method was like those produced using the melting method (a method used in the present study).

Also, the translucency values of barium disilicate-

based samples were measured to be close to those of lithium disilicate. This provides the dental sample a high translucency like a natural tooth [1]. The crack images were taken from the failed regions of the T0060 sample (heat treated at 773 K for 1h) due to the thermal shock test at different magnifications. The quenching test was carried out qualitatively. The surface cracking in the silicate-based dental ceramics with the quenching environment is explained by the generation of stress due to a mismatch between the crystalline and the amorphous phases in terms of the coefficient of thermal expansion. The crack initiation takes place at the stress concentration sites that are the weakest regions of the dental crowns although the crack initiation site was not observed on the crack surface. The thermal shock test introduced the surface cracking as can be seen in Fig. 4.

The part of the crack length within these intersection points is assumed to be only one crack (Fig. 4 a) and the radius of this single crack is the half of the length between two intersections whereas the orientation of this crack is described by the angles of  $\phi$  and  $\theta$  [35]. Fine perpendicular markings (red arrows) seen at a magnification of 1kx in Fig. 4 e and f were explained as the link up of crack segments and they were attributed to the presence of multiple crack planes [36, 37]. These fractographic features were also confirmed on the commercial IPS e.max CAD implant materials [38].

The barium disilicate sample showed a homogeneous structure (with low visible porosity) on the fracture surface. In the fracture images some voids (material defects) were observed that were found to be responsible for the crack nucleation as explained in a previous study [39].

As shown in Fig. 4 g and h, the fracture surface of our sample exhibited the regions of brittle fracture characteristics induced by the thermal shock. These

microstructural features resemble those observed in lithium disilicate [40]. The fracture zones in the SEM images of our samples were examined in terms of crack geometry and the lengths of the surface cracks (confined in a square).

The crack geometry was observed to be continuous and crack branching was not common across the fracture surface. At the tip of the cracks at the fracture surface a stress concentration takes place. That is why the dislocations of the chemical bonds tend to expand and result in the opening [41]. Further, the formation of the multiple cracks causes an interaction between them, consequently patterning the fracture surface.

However, these microstructures that contain low content of voids can be an alternative solution for the lithium disilicate dental materials against their chipping problem, which was dealt with in detail by a previous fractographic study [42].

The diffusion parameters of the dental material during the controlled crystallization process were calculated. As in Fig. 5 a, diffusivity ( $D$ ) of the diffused Ba cation vs treatment temperature indicated an exponential graph for our samples. Thus, the application of the nucleation treatment induced the formation of the main dental phase, barium disilicate. This graph was converted into the Arrhenius graph by considering the activation energy value, which is commonly used in the examinations of the glass-ceramic systems.

The diffusion rate-treatment temperature graph of the present system was found to be in good agreement with a linear Arrhenius graph.

The diffusivity values for Ba cation were obtained in the range of  $1 \times 10^{-15}$  and  $7 \times 10^{-15} \text{ cm}^2 \cdot \text{s}^{-1}$  in our study, which is good agreement with the values of Bocker's study [43] obtained in  $\text{Na}_2\text{O}-\text{K}_2\text{O}-\text{Al}_2\text{O}_3-\text{SiO}_2$  glass and Van Hoesen's study [44] obtained in  $5\text{BaO} \cdot 8\text{SiO}_2$  glass.

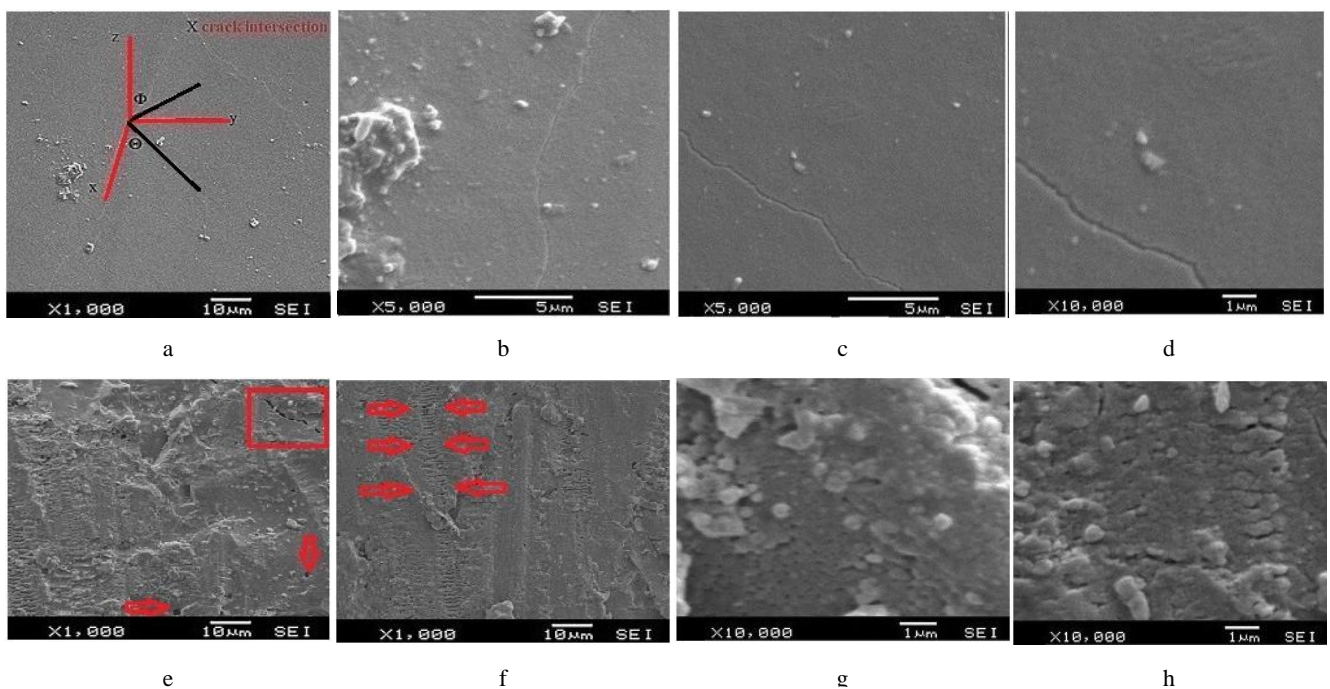
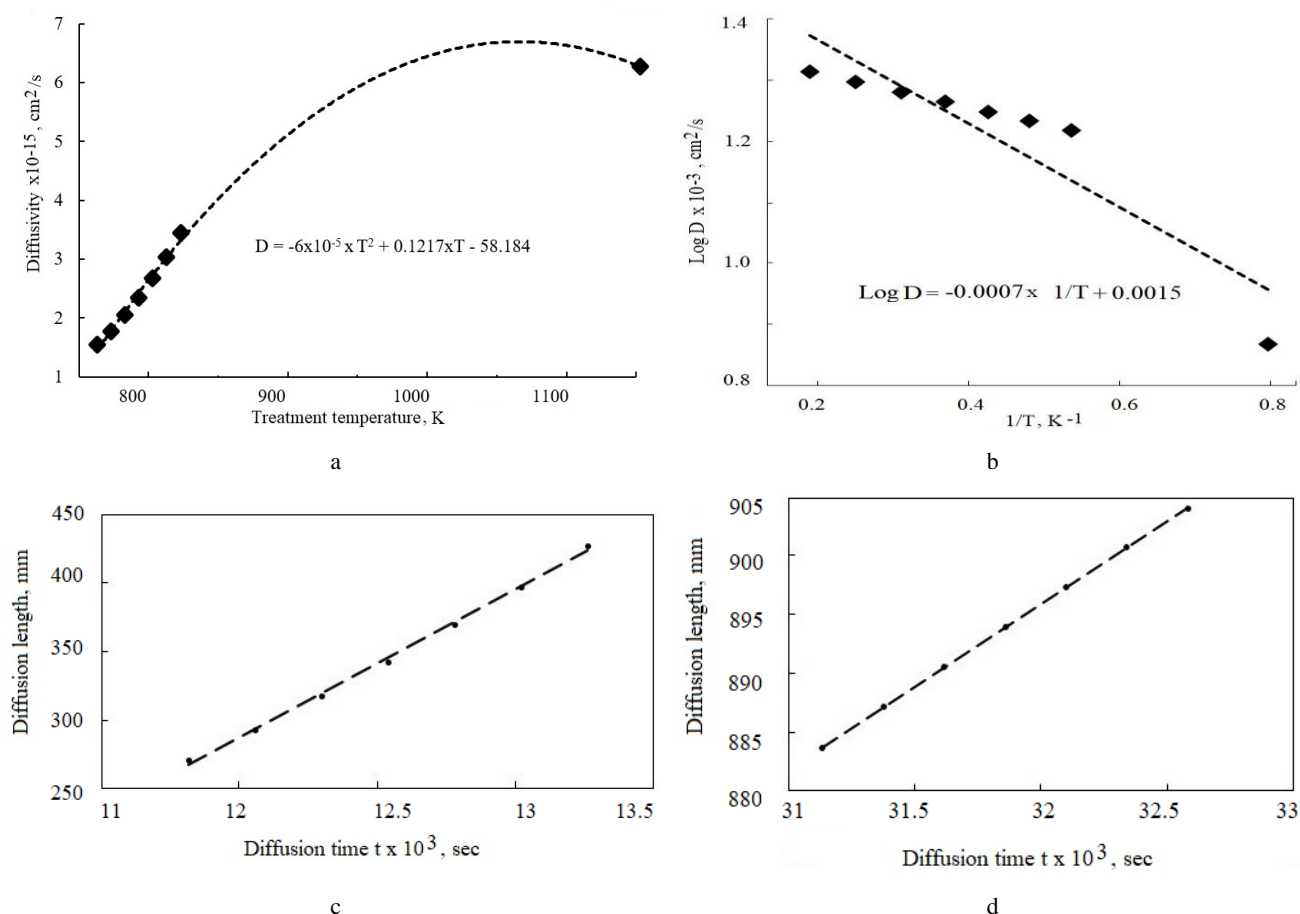


Fig. 4. Fracture surface of sample T0060 after thermal shock test



**Fig. 5.** Diffusion graphs: a–diffusivity-temperature; b–Arrhenius graph; Diffusion length-time graphs: c–after nucleation; d–crystallization treatments

On the other hand, Fokin [46] found diffusivity values for barium in the order of  $10^{-16} \text{ cm}^2 \cdot \text{s}^{-1}$  in  $\text{BaO} \cdot 2\text{SiO}_2$  glass, which are lower than our values. Grofmeier et al. [47] studied the barium diffusion in the mixed cation glasses and their diffusivity values were between  $10^{-10}$  and  $10^{-8} \text{ cm}^2 \cdot \text{s}^{-1}$ .

For calculating the diffusion length ( $L$ ) of this system, the parameter of diffusion time ( $t$ ) was utilized. Total diffusion time was determined by considering the heating time, nucleation temperatures (763–823 K), holding times (0.5–3 h) and the cooling time (down to room temperature). As in Fig. 5 c and d, when the crystallization treatment was applied to the samples, the sample length was approximately doubled.

However, when a single nucleation treatment was applied, the length values dropped nearly by half. The observed rise of the length values is related to the thermal diffusion of Ba cations into the quartz crystal. Both graphs indicated a linear relationship and the sample length ( $L$ ) increased monotonously with the diffusion time. The sample length values were determined to be 425 nm. and 900 nm. for only nucleation and the nucleation-crystallization cases respectively.

#### 4. CONCLUSIONS

In this study, the samples were prepared by the melt casting method. The diffusion and thermal shock

behaviour of the samples were examined. It was observed that barium disilicate dental samples had a similar crystalline structure and composition to the commercial lithium disilicates. XRD patterns of T4012 and T401 samples contained (101), (220) and (140) plane reflections corresponding to the highest peaks of the main crystalline phase. The content of the orthorhombic sanbornite phase increased with the treatment temperature. Early crystallization close to glass transition produced small crystallites without microstructural coarsening with temperature. According to surface examination after exposure to a qualitative quenching test, the fine perpendicular markings at the fracture surface were attributed to the presence of multiple crack planes. These features were in good agreement with those of commercial lithium disilicates. For our crystallized samples diffusivity ( $D$ ) of the Ba cation indicated an exponential behaviour. The diffusion rate-temperature graph of the present system was plotted, and it was in good agreement with the Arrhenius graph. The analysis results indicated that diffusion length ( $L$ ) was doubled after crystallization and the values were determined to be 425 nm. and 900 nm. for nucleated and crystallized samples respectively. According to the results obtained from the present study, we strongly believe that the outcomes obtained from this study will contribute to future work in terms of the clinical performance of these samples as promising materials for oral applications.

## Acknowledgments

This work has been technically supported by Dokuz Eylül University Industrial Service Department which provided the opportunity to obtain electron microscopy examinations. We thank Mr. Haluk Gürses for his contribution to the experimental work. Also, we particularly thank Prof. Ekrem Yanmaz from Department of Electrical and Electronics Engineering, Nişantaşı University for useful discussions on this study.

## REFERENCES

1. Wang, F., Gao, J., Wang, H., Chen, J.H. Flexural Strength and Translucent Characteristics of Lithium Disilicate Glass-Ceramics with Different P<sub>2</sub>O<sub>5</sub> Content *Materials & Design* 31 (7) 2010: pp. 3270–3274. <https://doi.org/10.1016/j.matdes.2010.02.013>
2. Kim, D., Kim, H.J., Yoo, S.I. Effects of Microstructures on the Mechanical Properties of Lithium Disilicate Glass-Ceramics for the SiO<sub>2</sub>-Li<sub>2</sub>O-P<sub>2</sub>O<sub>5</sub>-K<sub>2</sub>O-ZnO System *Materials Science and Engineering: A* 804 2021: pp. 140564. <https://doi.org/10.1016/j.msea.2020.140564>
3. May, J.T., Arata, A., Cook, N.B., Diefenderfer, K.E., Lima, N.B., Borges, A.L.S., Feitosa, S. Stepwise Stress Testing of Different CAD-CAM Lithium Disilicate Veneer Application Methods Applied to Lithium Disilicate Substructures *The Journal of Prosthetic Dentistry* Available online 14 July 2021. In Press. <https://doi.org/10.1016/j.prosdent.2020.05.033>
4. Meng, M., Wang, X.S., Li, K.Y., Deng, Z.X., Zhang, Z.Z., Sun, Y.L., Zhang, S.F., He, L., Guo, J.W. Effects of Surface Roughness on the Time-Dependent Wear Performance of Lithium Disilicate Glass Ceramic for Dental Applications *Journal of the Mechanical Behavior of Biomedical Materials* 121 2021: pp. 104638. <https://doi.org/10.1016/j.jmbbm.2021.104638>
5. Sultan, H., Balkaya, M.C. Clinical Success of Zirconia Based Restorations *Journal of Prosthodontics* 3 (2) 2017: pp. 113–119.
6. Akramin, M.R.M., Marizi, M.S., Husnain, M.N.M., Shaari, M.S. Analysis of Surface Crack Using Various Crack Growth Models *Journal of Physics: Conference Series* 1529 2020: pp. 042074. <https://doi.org/10.1088/1742-6596/1529/4/042074>
7. Simba, B.G., Ribeiro, M.V., Alves, M.F.R.P., Amarante, J.E.V., Strecker, K., dos Santos, C. Effect of the Temperature on the Mechanical Properties and Translucency of Lithium Silicate Dental Glass-ceramic *Ceramics International* 47 (7) Part A 2021: pp. 9933–9940. <https://doi.org/10.1016/j.ceramint.2020.12.137>
8. Lubauer, J., Belli, R., Petschelt, A., Cicconi, M.R., Hurle, K., Lohbauer, U. Concurrent Kinetics of Crystallization and Toughening in Multicomponent Biomedical SiO<sub>2</sub>-Li<sub>2</sub>O-P<sub>2</sub>O<sub>5</sub>-ZrO<sub>2</sub> Glass-ceramics *Journal of Non-Crystalline Solids* 554 2021: pp. 120607. <https://doi.org/10.1016/j.jnoncrysol.2020.120607>
9. Lien, W., Roberts, H.W., Platt, J.A., Vandewalle, K.S., Hill, T.J., Chu, T.M.G. Microstructural Evolution and Physical Behavior of a Lithium Disilicate Glass-ceramic *Dental Materials* 31 (8) 2015: pp. 928–940. <https://doi.org/10.1016/j.dental.2015.05.003>
10. El Batal, F., Azooz, M., Hamdy, Y. Preparation and Characterization of Some Multicomponent Silicate Glasses and Their Glass-Ceramics Derivatives for Dental Applications *Ceramics International* 35 2009: pp. 1211–1218. <https://doi.org/10.1016/j.ceramint.2008.06.009>
11. Goharian, P., Nemati, A., Shabanian, M., Afshar, A. Properties, Crystallization Mechanism and Microstructure of Lithium Disilicate Glass-ceramic *Journal of Non-Crystalline Solids* 356 2010: pp. 208–214. <https://doi.org/10.1016/j.jnoncrysol.2009.11.015>
12. Khalkhali, Z., Eftekhari Yekta, B., Marghussian, V.K. Preparation of Lithium Disilicate Glass-Ceramics as Dental Bridge Material *Journal of Ceramic Science and Technology* 5 2014: pp. 39–44. <https://doi.org/10.4416/JCST2013-00030>
13. Apel, E., van't Hoen, C., Rheinberger, V., Höland, W. Influence of ZrO<sub>2</sub> on the Crystallization and Properties of Lithium Disilicate Glass-Ceramics Derived from a Multi-Component System *Journal of the European Ceramic Society* 27 (2–3) 2007: pp. 1571–1577. <https://doi.org/10.1016/j.jeurceramsoc.2006.04.103>
14. da R. Fernandes, H.A.G. Development of Lithium Disilicate Based Glassceramics. Department of Materials and Ceramics Engineering. Ph.D Thesis, University of Aveiro (Portugal), 2012.
15. Höland, W., Apel, E., vant Hoen, C., Rheinberger, V. Studies of Crystal Phase Formations in High-Strength Lithium Disilicate Glass-ceramics *Journal of Non-Crystalline Solids* 352 2006: pp. 4041–4050. <https://doi.org/10.1016/j.jnoncrysol.2006.06.039>
16. Soares, R.S., Monteiro, R.C.C., Lima, M.M.R.A., Silva, R.J.C. Crystallization of Lithium Disilicate-Based Multicomponent Glasses-Effect of Silica/Lithia Ratio *Ceramics International* 41 (1) Part A 2015: pp. 317–324. <https://doi.org/10.1016/j.ceramint.2014.08.074>
17. Wang, F., Chai, Z., Deng, Z., Gao, J., Wang, H., Chen, J. Effect of Heat-Pressing Temperature and Holding Time on the Microstructure and Flexural Strength of Lithium Disilicate Glass-Ceramics *PLOS ONE* 10 (6) 2015: pp. e0130919. <https://doi.org/10.1371/journal.pone.0130919>
18. Tulyaganov, D.U., Agathopoulos, S., Kansal, I., Valerio, P., Ribeiro, M.J., Ferreira, J.M.F. Synthesis and Properties of Lithium Disilicate Glass-Ceramics in the System SiO<sub>2</sub>-Al<sub>2</sub>O<sub>3</sub>-K<sub>2</sub>O-Li<sub>2</sub>O *Ceramics International* 35 2009: pp. 3013–3019. <https://doi.org/10.1016/j.ceramint.2009.04.002>
19. Wen, G., Zheng, X., Song, L. Effects of P<sub>2</sub>O<sub>5</sub> and Sintering Temperature on Microstructure and Mechanical Properties of Lithium Disilicate Glass-ceramics *Acta Materialia* 55 (10) 2007: pp. 3583–3591. <https://doi.org/10.1016/j.actamat.2007.02.009>
20. Molla, A.R., Chakradhar, R.P.S., Kesavulu, C.R., Rao, J.L., Biswas, S.K. Microstructure, Mechanical, EPR and Optical Properties of Lithium Disilicate Glasses and Glass-ceramics doped with Mn<sup>2+</sup> Ions *Journal of Alloys and Compounds* 512 (1) 2012: pp. 105–114. <https://doi.org/10.1016/j.jallcom.2011.09.031>
21. Zheng, X., Wen, G., Song, L., Huang, X.X. Effects of P<sub>2</sub>O<sub>5</sub> and Heat Treatment on Crystallization and Microstructure in Lithium Disilicate Glass Ceramics *Acta Materialia* 56 (3) 2008: pp. 549–558. <https://doi.org/10.1016/j.actamat.2007.10.024>
22. Albakry, M., Guazzato, M., Swain, M.V. Fracture

- Toughness and Hardness Evaluation of Three Pressable All-Ceramic Dental Materials *Journal of Dentistry* 31 2003: pp. 181–188.  
[https://doi.org/10.1016/s0300-5712\(03\)00025-3](https://doi.org/10.1016/s0300-5712(03)00025-3)
23. Aquilanti, V., Coutinho, N.D., Carvalho-Silva, V.H. Kinetics of Low-Temperature Transitions and a Reaction Rate Theory From Non-Equilibrium Distributions *Philosophical Transactions of the Royal Society A* 375 2017: pp. 1–20.  
<https://doi.org/10.1098/rsta.2016.0201>
  24. Kingery, W.D., Bowen, H.K., Uhlmann, D.R. Introduction To Ceramics 2nd Edition Wiley New York, 1976.
  25. Barsoum, M. Fundamentals of Ceramics *CRC Press*, 2020.
  26. Atila, A., Ouaskit, S., Hasnaoui, A. Ionic Self-Diffusion and the Glass Transition Anomaly in Aluminosilicates *Physical Chemistry Chemical Physics* 22 (30) 2020: pp. 17205–17212.  
<https://doi.org/10.1039/D0CP02910F>
  27. Mehrer, H. Diffusion in Solids: Fundamentals, Methods, Materials, Diffusion-Controlled Processes, 2007 Springer Berlin.
  28. Wu, X. Diffusion of Sodium in Mixed Glass Former Oxide Glasses Ph.D Dissertation Cornell University, 2012.
  29. Mehrer, H. Diffusion in Ion-conducting Oxide Glasses and in Glassy Metals *Zeitschrift für Physikalische Chemie* 223 (10–11) 2009: pp. 1143–1160.  
<https://doi.org/10.1524/zpch.2009.6070>
  30. Mehrer, H., Imre, A.W., Nijokop, E.T. Diffusion and Ionic Conduction in Oxide Glasses *The Second International Symposium on Atomic Technology-IOP Publishing Journal of Physics: Conference Series* 106 2008: pp. 012001.  
<https://doi.org/10.1088/1742-6596/106/1/012001>
  31. Greaves, G.N., Gurman, S.J., Catlow, C.R.A., Chadwick, A.V., Houde Walter, S., Henderson, C.M.B., Dobson, B.R. A Structural Basis For Ionic Diffusion In Oxide Glasses *Philosophical Magazine A* 64 (5) 1991: pp. 1059-1072.  
<http://dx.doi.org/10.1080/01418619108204878>
  32. Heitjans, P., Indris, S. Diffusion and Ionic Conduction In Nanocrystalline Ceramics *Journal of Physics: Condensed Matter* 15 (30) 2003: pp. R1257.  
<https://doi.org/10.1557/PROC-676-Y6.6>
  33. AMAT Homepage. Diffusion, Intitute for Material Science, Faculty of Engineering, University of Kiel. 15 February 2021. Available from:  
<https://www.tf.uni-kiel.de/matwis/amat/>
  34. Puig, J., Ansart, F., Lenormand, P., Antoine, L., Dailly, J. Sol-gel Synthesis and Characterization of Barium (Magnesium) Aluminosilicate Glass Sealants for Solid Oxide Fuel Cells *Journal of Non-Crystalline Solids* 357 (19–20) 2011: pp. 3490–3494.  
<https://doi.org/10.1016/j.jnoncrysol.2011.06.025>
  35. Mallet, C., Fortin, J., Gueguen, Y., Bouyer, F. Evolution of the Crack Network in Glass Samples Submitted to Brittle Creep Conditions *International Journal of Fracture* 190 2014: pp. 111–124.  
<https://doi.org/10.1007/s10704-014-9978-9>
  36. Scherrer, S.S., Quinn, J.B., Quinn, G.D., Wiskott, H.W.A. Fractographic Ceramic Failure Analysis Using the Replica Technique *Dental Materials* 23 (11) 2007: pp. 1397–1404.  
<https://doi.org/10.1016/j.dental.2006.12.002>
  37. Gonzaga, C.C., Cesar, P.F., Miranda, Jr.W.G., Yoshimura, H.N. Slow Crack Growth And Reliability Of Dental Ceramics *Dental Materials* 27 2011: pp. 394–406.  
<https://doi.org/10.1016/j.dental.2010.10.025>
  38. Jalali, H., Bahrani, Z., Zeighami, S. Effect of Repeated Firings on Microtensile Bond Strength of Bi-Layered Lithium Disilicate Ceramics (e.max CAD and e.max Press) *The Journal of Contemporary Dental Practice* 17 (7) 2016: pp. 530–535.
  39. Dapieve, K.S., Machry, R.V., Pilecco, R.O., Kleverlaan, C.J., Pereira, G.K.R., Venturini, A.B., Valandro, L.F. One-Step Ceramic Primer as Surface Conditioner: Effect on the Load-Bearing Capacity Under Fatigue of Bonded Lithium Disilicate Ceramic Simplified Restorations *Journal of the Mechanical Behavior of Biomedical Materials* 104 2020: pp. 103686.  
<https://doi.org/10.1016/j.jmbbm.2020.103686>
  40. Oilo, M., Hardang, A.D., Ulsund, A.H., Gjerdet, N.R. Fractographic Features of Glass-Ceramic and Zirconia-Based Dental Restorations Fractured During Clinical Function *European Journal of Oral Sciences* 122 (3) 2014: pp. 238–44.  
<https://doi.org/10.1111/eos.12127>
  41. Huang, S., Cao, P., Wang, C., Huang, Z., Gao, W. Fabrication of a High-Strength Lithium Disilicate Glass-Ceramic in a Complex Glass System *Journal of Asian Ceramic Societies* 1 2013: pp. 46–52.  
<https://doi.org/10.1016/j.jascer.2013.02.007>
  42. Gross, D., Seelig, T. Fracture Mechanics: with an Introduction to Micromechanics *Springer*, 2011.
  43. Bocker, C., Avramov, I., Rüssel, C. Viscosity and Diffusion of Barium and Fluoride in Na<sub>2</sub>O/K<sub>2</sub>O/Al<sub>2</sub>O<sub>3</sub>/SiO<sub>2</sub>/BaF<sub>2</sub> Glasses *Chemical Physics* 369 2010: pp. 96–100.  
<https://doi.org/10.1016/j.chemphys.2010.03.010>
  44. Van Hoesen, D.C., Xia, X., McKenzie, M.E., Kelton, K.F. Crystallization Kinetics in a 5BaO·8SiO<sub>2</sub> Glass *Journal of Non-Crystalline Solids* 553 2021: pp. 120479.  
<https://doi.org/10.1016/j.jnoncrysol.2020.120479>
  45. Kumar, S., Mishra, R.K., Tomar, B.S., Tyagi, A.K., Kaushik, C.P., Raj, K., Manchanda, V.K. Heavy Ion Rutherford Backscattering Spectrometry (HIRBS) Study of Barium Diffusion in Borosilicate Glass *Nuclear Instruments and Methods in Physics Research B* 266 2008: pp. 649–652.  
<https://doi.org/10.1016/j.nimb.2007.12.062>
  46. Fokin, V.M., Abyzov, A.S., Rodrigues, A.M., Pompermayer, R.Z., Macena, G.S., Zanotto, E.D., Ferreira, E.B. Effect of Non-Stoichiometry On The Crystal Nucleation and Growth In Oxide Glasses *Acta Materialia* 180 2019: pp. 317–328.  
<https://doi.org/10.1016/j.actamat.2019.09.017>
  47. Grofmeier, M., Natrup, F.V., Bracht, H. Barium Diffusion in Mixed Cation Glasses *Physical Chemistry Chemical Physics* 9 2007: pp. 5822–5827.  
<https://doi.org/10.1039/b709868e>

